

# Functional evaluation of artificial skeletal muscle tissue constructs fabricated by a magnetic force-based tissue engineering technique

Yamamoto, Yasunori  
Graduate School of Systems Life Sciences, Kyushu University

Ito, Akira  
Department of Chemical Engineering, Faculty of Engineering, Kyushu University

Fujita, Hideaki  
Toyota Central R and D Laboratories, Inc.

Nagamori, Eiji  
Toyota Central R and D Laboratories, Inc.

他

<https://hdl.handle.net/2324/25538>

---

出版情報 : Tissue Engineering Part A. 17 (1/2), pp.107-114, 2011-01. Mary Ann Liebert  
バージョン :  
権利関係 : (C) Mary Ann Liebert, Inc.



# Functional Evaluation of Artificial Skeletal Muscle Tissue Constructs Fabricated by a Magnetic Force-Based Tissue Engineering Technique

Yasunori Yamamoto, M. Eng.,<sup>1</sup> Akira Ito, Ph.D.,<sup>2</sup> Hideaki Fujita, Ph.D.,<sup>3</sup>  
Eiji Nagamori, Ph.D.,<sup>3</sup> Yoshinori Kawabe, Ph.D.,<sup>2</sup> and Masamichi Kamihira, Ph.D.<sup>1,2</sup>

Skeletal muscle tissue engineering is currently applied in a variety of research fields, including regenerative medicine, drug screening, and bioactuator development, all of which require the fabrication of biomimetic and functional skeletal muscle tissues. In the present study, magnetite cationic liposomes were used to magnetically label C2C12 myoblast cells for the construction of three-dimensional artificial skeletal muscle tissues by an applied magnetic force. Skeletal muscle functions, such as biochemical and contractile properties, were evaluated for the artificial tissue constructs. Histological studies revealed that elongated and multinucleated myotubes were observed within the tissue. Expression of muscle-specific markers, such as myogenin, myosin heavy chain and tropomyosin, were detected in the tissue constructs by western blot analysis. Further, creatine kinase activity increased during differentiation. In response to electric pulses, the artificial tissue constructs contracted to generate a physical force (the maximum twitch force, 33.2  $\mu\text{N}$  [1.06  $\text{mN}/\text{mm}^2$ ]). Rheobase and chronaxie of the tissue were determined as 4.45 V and 0.72 ms, respectively. These results indicate that the artificial skeletal muscle tissue constructs fabricated in this study were physiologically functional and the data obtained for the evaluation of their functional properties may provide useful information for future skeletal muscle tissue engineering studies.

## Introduction

**T**ISSUE-ENGINEERED SKELETAL MUSCLE is used in a variety of research fields, including regenerative medicine, drug screening, and bioactuator development. In regenerative medicine, they are employed in the treatment of traumatic injury, tumor ablation, and muscular dystrophy.<sup>1</sup> Natural skeletal muscle tissue is composed of striated myotubes arranged in parallel alignment. A connective tissue covering, predominantly composed of collagen, tethers adjacent myotubes to form individual muscle fibers. In addition to muscle fibers, satellite cells located beneath the basal lamina, at the periphery of muscle fibers, are believed to play an important role in the repair and replacement of damaged skeletal muscle cells.<sup>2</sup> Thus, it has been proposed that satellite cells are key to the successful engineering of skeletal muscle tissue.<sup>3</sup> In drug screening, tissue-engineered skeletal muscle is very useful tool for evaluating the toxicity and efficacy of drugs and the development of new drug targets. *In vitro* experiments using cell culture systems are an extremely useful approach that can be used in place of animal models,

thereby limiting the number of animals used. Myoblast cell lines derived from satellite cells, including mouse C2C12 cells, have been applied as an excellent model for the construction of skeletal muscle, as they proliferate indefinitely in the mitotic phase and can be differentiated into multinucleated myotubes.<sup>4</sup> The use of established cell lines has numerous benefits in drug screening and evaluation. They provide repeatable and reproducible systems for the development and testing of new and existing drugs, without the major ethical concerns involved with animal studies, and provide model systems for the analysis of gene modifications on promoting improved cell functions.

In recent years, skeletal muscle tissues have attracted much attention as bioactuators. Herr and Dennis designed a swimming robot using frog semitendinosus muscle and proposed a muscle-powered actuator.<sup>5</sup> Morishima *et al.* demonstrated a biomicroactuator using cultured rat primary neonatal cardiomyocytes to drive polymer micropillars.<sup>6</sup> Further, a bioactuator powered by insect dorsal vessel tissue, which was capable of performing for extended periods of time at room temperature without maintenance, has also

<sup>1</sup>Graduate School of Systems Life Sciences and <sup>2</sup>Department of Chemical Engineering, Faculty of Engineering, Kyushu University, Fukuoka, Japan.

<sup>3</sup>Toyota Central R&D Laboratories, Inc., Aichi, Japan.

been demonstrated.<sup>7</sup> Through the exploitation of cell micropatterning techniques, Feinberg *et al.* fabricated muscle thin films using polydimethylsiloxane and cardiomyocytes for the construction of actuators and power devices.<sup>8</sup> Tanaka *et al.* created an on-chip cellular micropump, using cardiomyocyte sheets as a prototype of applicative biomiocroactuators.<sup>9</sup>

The fabrication of tissue-engineered skeletal muscles that are capable of imitating natural skeletal muscle is believed to be crucial for the development of numerous therapies with a variety of applications. As muscle differentiation has been shown to be promoted in the presence of extracellular matrix (ECM) proteins such as collagen and laminin, collagen,<sup>3,10</sup> and/or Matrigel<sup>11</sup> have been used in the fabrication of artificial muscle tissue constructs. Although collagen has been used as a cell scaffold, to define the size and shape of construct, hard matrix constructs may interfere with the force generation of myotubes. Dennis *et al.* have succeeded in fabricating a scaffold-free skeletal muscle tissue, which they designated myooid, by the self-dissociation of a monolayer myoblast cell sheet from the culture surface, which is subsequently followed by self-organization.<sup>12</sup> However, scaffold-free tissue-engineered skeletal muscle constructs should be fixed to tendon-like anchors to prevent shrinking and induce orientation within the tissue during myogenic differentiation *in vitro*. Laminin-coated silk-suture anchors were used as an artificial tendon for the myooids.<sup>12</sup> In contrast, we previously developed a tissue engineering technique designated magnetic force-based tissue engineering (Mag-TE), in which cells labeled with functionalized magnetic nanoparticles were used to fabricate tissue constructs by applying a magnetic force.<sup>13,14</sup> Further, we have applied this technique for the fabrication of artificial skeletal muscle tissue.<sup>15,16</sup> C2C12 cells, magnetically labeled with magnetite cationic liposomes (MCLs), were added into the well of a culture dish containing a polycarbonate cylinder fixed to the center of the well. The cells were forced to accumulate onto an ultralow attachment surface using a magnet. During the cultivation, the cell layer compressed toward the cylinder, resulting in the formation of a ring-shaped tissue construct, possessing a high cell-dense population with an oriented multilayered structure.<sup>15</sup>

The functional comparison of artificial skeletal muscle tissue constructs to natural skeletal muscle is extremely important for the practical application of the artificial tissue. However, very few systematic and quantitative evaluations have attempted to characterize the biochemical and contractile properties of tissue-engineered skeletal muscle. Thus, the main focus of the present study was to characterize the biochemical and contractile properties of artificial skeletal muscle tissue, fabricated by Mag-TE. Our results will provide useful information for skeletal muscle tissue engineering.

## Materials and Methods

### Cell culture

Mouse C2C12 myoblast cells were grown in Dulbecco's modified Eagle's medium, supplemented with 10% fetal bovine serum, 100 U/mL penicillin G potassium, and 0.1 mg/mL streptomycin sulfate. Cells were cultured at 37°C in a 5% CO<sub>2</sub> incubator.

### Preparation of MCLs

MCLs were prepared from colloidal magnetite and a lipid mixture consisting of *N*-( $\alpha$ -trimethylammonioacetyl)-dodecyl-D-glutamate chloride, dilauroylphosphatidylcholine, and dioleoylphosphatidyl-ethanolamine, in a molar ratio of 1:2:2, as previously described.<sup>17</sup> The magnetite particles (Fe<sub>3</sub>O<sub>4</sub>; average particle size, 10 nm) were purchased from Toda Kogyo (Hiroshima, Japan). The magnetic characteristics at 796 kA/m (room temperature) were as follows: 2.0 kA/m coercivity; 63.9 Am<sup>2</sup>/kg saturation flux density; and 2.6 Am<sup>2</sup>/kg remanent flux density.

### Fabrication of skeletal muscle tissue constructs by Mag-TE

To magnetically label the C2C12 cells,  $7 \times 10^5$  cells were seeded in 100-mm tissue culture dishes (Greiner Bio-One, Frickenhausen, Germany) containing 10 mL of the culture medium, in the presence of MCLs (net magnetite concentration, 100 pg/cell), and incubated for 8 h to allow for MCL uptake.

The artificial skeletal muscle tissue constructs were prepared as previously described,<sup>15</sup> with slight modifications. Briefly, a polycarbonate cylinder (diameter, 12 mm) was fixed at the center of the well of a 24-well ultralow-attachment culture plate (culture area, 200 mm<sup>2</sup>/well; Corning, New York, NY). MCL-labeled C2C12 cells ( $1 \times 10^6$  cells) were seeded into the gap between the well wall and the polycarbonate cylinder, and a cylindrical neodymium magnet (diameter, 30 mm; height, 15 mm; magnetic induction, 0.4 T) was placed under the well. Subsequently, the cells were cultured for 2 days to allow for the formation of a ring-shaped cellular construct. After 2-day culture in the standard growth medium, 0.1 mL of an ECM solution, consisting of 0.04 mL of type I collagen (1.1 mg/mL; Nitta Gelatin, Osaka, Japan), 0.01 mL of the growth medium, and 0.05 mL of Matrigel (4.4 mg/mL; BD Biosciences, Franklin Lakes, NJ), was added to the well and the solution was subsequently replaced with the culture medium. After 4 h, the cellular ring was removed from the polycarbonate cylinder and hooked around two stainless-steel minuten pins (0.3 mm diameter; Shiga, Tokyo, Japan), fixed 8 mm apart from one another on a silicone rubber sheet in a 35-mm culture dish. To induce myogenic differentiation, the cellular rings were cultured in the differentiation medium consisting of Dulbecco's modified Eagle's medium supplemented with 0.4% Ultrosor G (Pall, East Hills, NY), 100 U/mL penicillin G potassium, and 0.1 mg/mL streptomycin sulfate.

### Histological study

Before histological evaluation, tissues were washed three times with phosphate-buffered saline (PBS), fixed in 4% paraformaldehyde (PFA) in PBS, and embedded in paraffin. Thin sections (4  $\mu$ m) were prepared and stained with hematoxylin and eosin, and subsequently observed under a BZ-9000 microscope (Keyence, Tokyo, Japan). Before immunostaining, tissues were washed with PBS and fixed in 4% PFA for 15 min. They were then skinned in PBS containing 0.2% Triton-X 100 for 15 min, washed three times with PBS, and blocked in PBS containing 1% (w/v) bovine serum albumin for 30 min. The specimens were labeled with

a primary antibody against  $\alpha$ -actinin (A-7811, monoclonal anti- $\alpha$ -actinin EA-53; Sigma-Aldrich, St. Louis, MO) for 45 min. Then, they were washed three times with PBS and immersed in PBS containing 1% bovine serum albumin, an Alexa488-conjugated secondary antibody, Alexa546-phalloidin, and 4', 6-diamidino-2-phenylindole (DAPI) for 45 min. All fluorescent probes used in this study were purchased from Invitrogen (Carlsbad, CA). The specimens were washed three times with PBS and observed under a BZ-9000 fluorescence microscope (Keyence).

#### *Measurement of total cell nuclei*

Artificial tissue constructs were washed with PBS and the total number of nuclei was counted using NucleoCassette™ (Chemometec, Allerød, Denmark) and NucleoCounter™ (Chemometec). Total protein concentration was determined by bicinchoninic acid assay.

#### *Western blot analysis*

Cellular proteins were extracted from the artificial tissues by a homogenization and freeze-thawing method. Protein samples (30  $\mu$ g) were mixed with SDS-PAGE sample buffer containing 2-mercaptoethanol and boiled at 100°C for 5 min. Subsequently, the samples were electrophoresed on a 7.5% (for myosin heavy chain [MHC]) or 12% (for myogenin, tropomyosin, and GAPDH) acrylamide gel and the proteins were then transferred to a polyvinylidene-fluoride membrane (GE Healthcare, Buckinghamshire, United Kingdom). After blocking using 5% skimmed milk in Tris-buffered saline containing 0.05% Tween 20 at 4°C overnight, the membrane was incubated with the primary antibody (anti-myogenin [ab1835; Abcam, Cambridge, United Kingdom], anti-MHC [sc20641; Santa Cruz Biotechnology, Santa Cruz, CA], anti-tropomyosin [ab7785; Abcam], or anti-GAPDH [Cell Signaling Technology, Danvers, MA]) for 1 h. The specific antibodies were detected using horseradish peroxidase-conjugated secondary antibodies (Santa Cruz Biotechnology) and a chemiluminescence detection kit (ECL detection system; GE Healthcare).

#### *Creatine kinase activity*

The artificial tissue constructs were rinsed with PBS and homogenized in cell lysis buffer containing 1 M NaCl, 1 mM EDTA, 1% Triton X-100, and 10 mM Tris-HCl (pH 7.2).<sup>18</sup> The lysates were stored at -80°C until use. Creatine kinase activity of the samples was determined with a commercial assay kit (Wako Pure Chemical Industries, Tokyo, Japan).

#### *Tension measurement*

Carbon electrodes were placed 18 mm apart at opposite sides of a tissue culture plate. An artificial tissue ring was hooked around two stainless-steel minuten pins (0.3 mm diameter; Shiga). One pin was attached to a force transducer (AE-801; SonorOne, Sausalito, CA) and the other was fixed to the silicon rubber sheet placed on the bottom of the culture plate. During testing, the medium was maintained at 30°C–32°C, using a heated aluminum platform (HI-1000; AsOne, Osaka, Japan). Electric pulses were controlled by a personal computer with specially designed LabView software (National Instruments, Austin, TX), and the applied electric

pulse and measured force were recorded using the same computer. When measuring twitch contraction, the tissue sample was stimulated with an electric pulse of 15 V, with a width of 10 ms, whereas when measuring tetanic contraction, the tissue sample was stimulated with electric pulse with the following properties: voltage, 15 V; width, 10 ms; frequency, 50 Hz; duration, 2 s. Tissue sample excitability was measured by first applying a 10-ms single stimulus pulse while adjusting the stimulus intensity to achieve a force of 50% peak twitch force (Pt). The resulting voltage required to elicit a 50% Pt was defined as rheobase.<sup>12</sup> The stimulus intensity was then fixed to twofold of the rheobase value and the stimulus duration was adjusted until twitch forces of 50% Pt were reached once again. The resulting stimulus duration was defined as chronaxie.<sup>12</sup> Frequency properties of the tissue sample were evaluated by applying electric pulses (voltage, 15 V; width, 10 ms; train duration, 10 s) with various frequencies in the range of 0.2–50 Hz.

#### *Statistical analysis*

Statistical comparisons were evaluated using the Mann-Whitney rank sum test, and the values of  $p < 0.05$  were considered to be significant different.

## **Results and Discussion**

#### *Histological observation of artificial skeletal muscle tissues*

The MCL concentration (100 pg/cell) used for the magnetic labeling of C2C12 cells had been previously optimized by our group in another study.<sup>15,19</sup> Using the optimal concentration, MCL uptake reached 9.4 pg-magnetite per cell after 8-h incubation, and the magnetic labeling of C2C12 cells with MCLs (100 pg/cell) did not affect cell viability and differentiation (data not shown). When the MCL-labeled C2C12 cells were seeded into a well with a polycarbonate cylinder fixed to the center, the cells were uniformly accumulated to the bottom of the well by applying magnetic force (Fig. 1A). When the cell sheet was further cultured in the growth medium for 2 days, the sheet contracted drastically to form a ring-like tissue construct surrounding the cylinder (Fig. 1B). In the absence of the magnetic force, the cells did not form a tissue construct (data not shown), suggesting that the magnetic accumulation of the cells induced self-organization to form a cell sheet, eventually resulting in the formation of a tissue ring. After 2-day culture in the growth medium, the tissue ring was coated with ECM, composed of type I collagen and Matrigel, detached from the cylinder and transferred to a 35-mm tissue culture dish. As shown in Figure 1C, the tissue ring was hooked around two anchor pins placed 8 mm apart and cultured in the differentiation medium. Histological examination of the tissue ring revealed that the cells within the tissue construct formed multinucleated myotubes, which were aligned in parallel to the circumference direction of the cylinder (Fig. 1D). To further evaluate differentiation of the tissue ring, the cells in the tissue were stained with specific antibodies against  $\alpha$ -actinin and actin filament. As shown in Figure 1E, sarcomere structures were observed in the tissue construct. These results indicate that C2C12 cells successfully differentiated into skeletal muscle cells within the ring-shaped tissue construct.

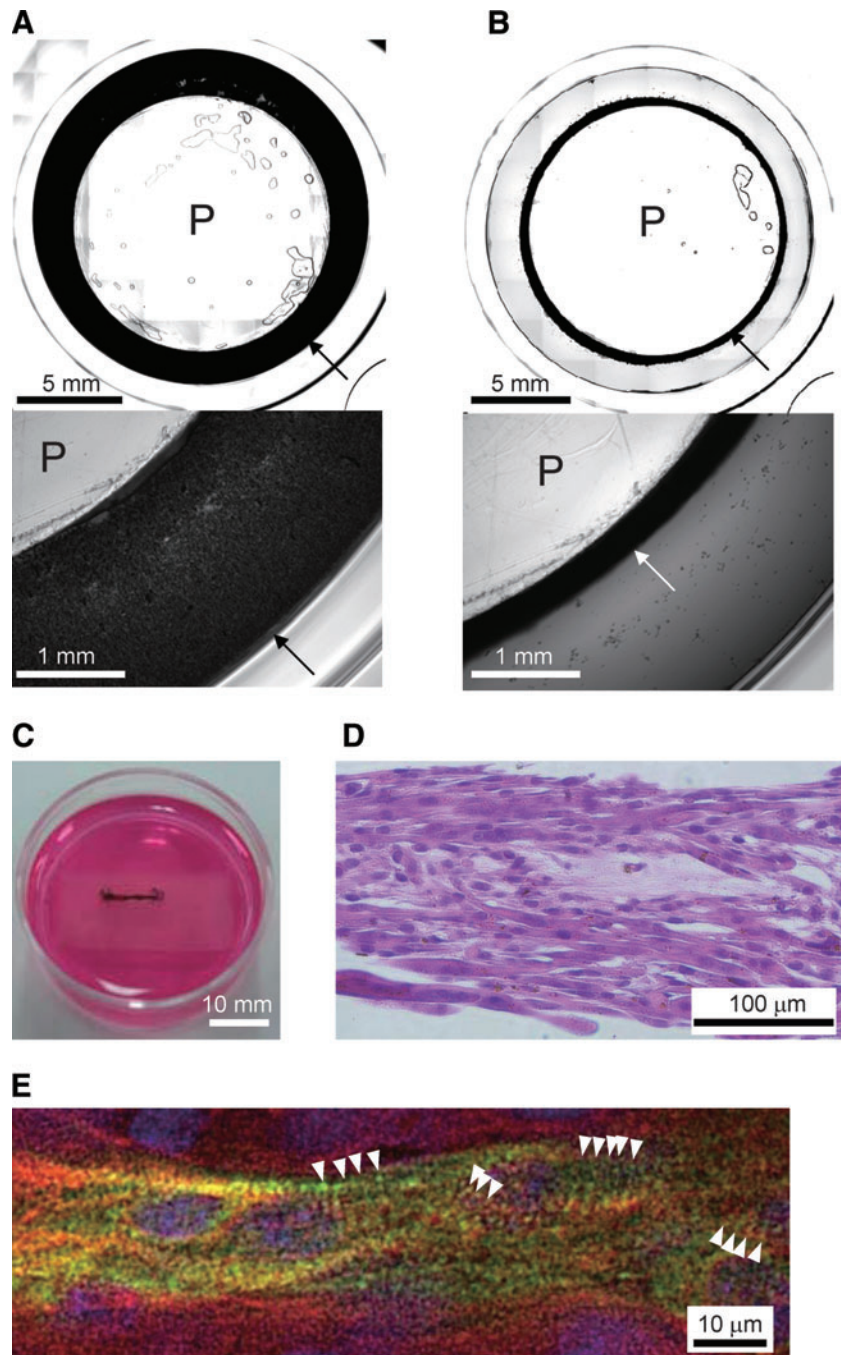


**FIG. 1.** Observation of artificial tissue constructs fabricated by magnetic force-based tissue engineering. **(A, B)** Bright-field micrographs of magnetite cationic liposomes-labeled C2C12 cell layers, under a magnetic force for 1 h **(A)** and 12 h **(B)** after seeding. The cell layer gradually contracted toward the polycarbonate cylinder (P), resulting in the formation of a ring-shaped tissue construct (arrows). **(C)** A bright-field photograph of an artificial tissue construct at day 17 in the differentiation medium. **(D)** A bright-field micrograph of a hematoxylin and eosin-stained section of the artificial tissue construct at day 7. **(E)** Immunostaining of the artificial tissue construct for  $\alpha$ -actinin (green) and F-actin (red). Cell nuclei were stained with 4', 6-diamidino-2-phenylindole (DAPI; blue). Arrowheads indicate the sarcomere structures. Color images available online at [www.liebertonline.com/ten](http://www.liebertonline.com/ten).

Figure 2A shows the number of cell nuclei within the tissue construct during the differentiation culture. After 2-day culture in the growth medium (day 0), the number of nuclei within the tissue construct was  $1.0 \times 10^6$ , which was the same as the initial cell density, suggesting that cell proliferation did not occur after tissue organization. When the tissue construct was cultured in the differentiation medium, the number of nuclei markedly decreased from days 2 to 7, after which it maintained itself at a steady state of  $\sim 2 \times 10^5$  cell nuclei. As no distinct necrotic area was observed within the tissue construct (Fig. 1D), and oxygen and nutrients were not limiting factors in the culture conditions of tissue constructs with  $<200$ - $\mu\text{m}$  thickness, we proposed that the

decrease in total nuclei of the tissue construct was the result of programmed cell death, which is a characteristic of skeletal muscle development. During the differentiation of muscle cells, subpopulations of myoblasts undergo apoptosis during myoblast fusion.<sup>20</sup> We also detected apoptotic cells in the tissue constructs on day 7 by the TUNEL assay, and the apoptotic cell death during differentiation was not caused by MCL labeling of cells (data not shown). Conversely, the amount of total protein per cell nucleus increased from days 2 to 7 and was also subsequently maintained at a constant level (Fig. 2B). Thus, we further analyzed the expression level of muscle differentiation marker proteins.

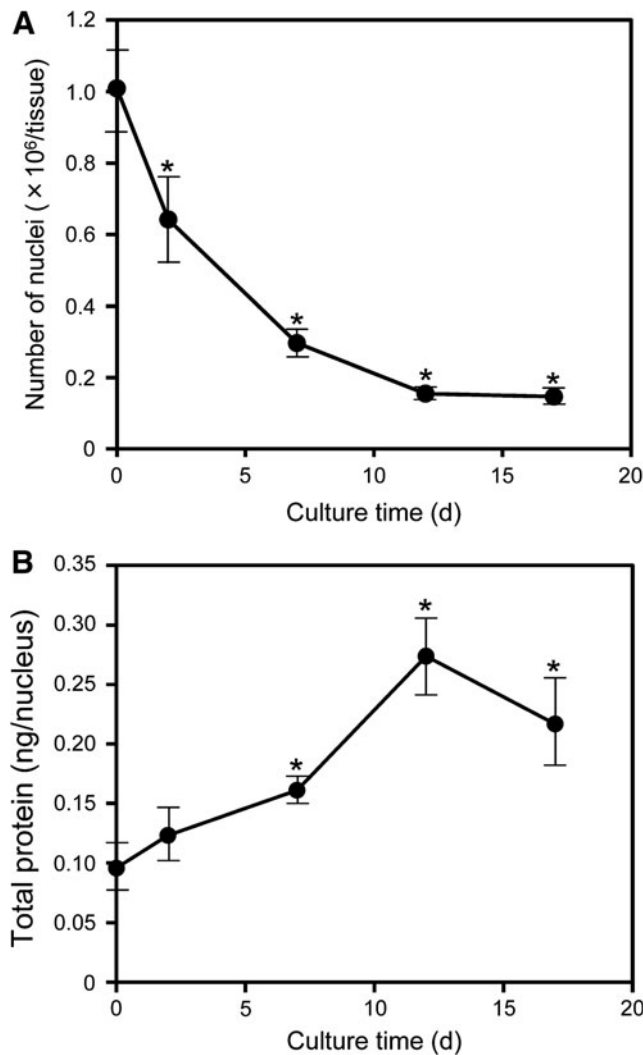


**FIG. 2.** Total cell nuclei and protein concentrations in artificial tissue constructs during differentiation. **(A)** Number of cell nuclei. The data are expressed as mean  $\pm$  SD of three constructs. \* $p < 0.05$  against day 0. **(B)** Total protein per cell nucleus. The data are expressed as mean  $\pm$  SD of three constructs. \* $p < 0.05$  against day 0.

#### Biochemical analyses of artificial skeletal muscle tissues

To evaluate skeletal muscle differentiation, the expression levels of myogenin, MHC, and tropomyosin were measured in the artificial tissue constructs by western blot analysis (Fig. 3A). Myogenin expression increased after 2-day culture in the differentiation medium and was thereafter maintained at a low level. Myogenin is a transcription factor and early marker in the differentiation of myoblasts, that plays a crucial role in muscle fusion and myotube formation.<sup>21</sup> These results were consistent with previous observations. The expression levels of the later-stage muscle-specific proteins,<sup>22</sup> MHC, and tropomyosin, increased from day 2 and then maintained at high levels throughout the culture period. These results indicate that muscle differentiation of the artificial tissue constructs began at day 2, with an increase of muscle-specific protein expression, even though the total

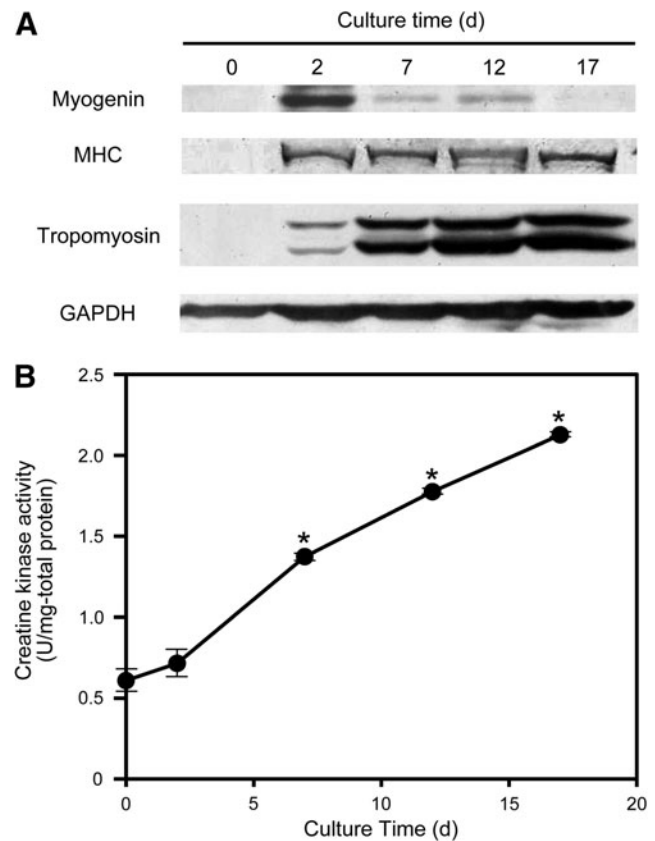


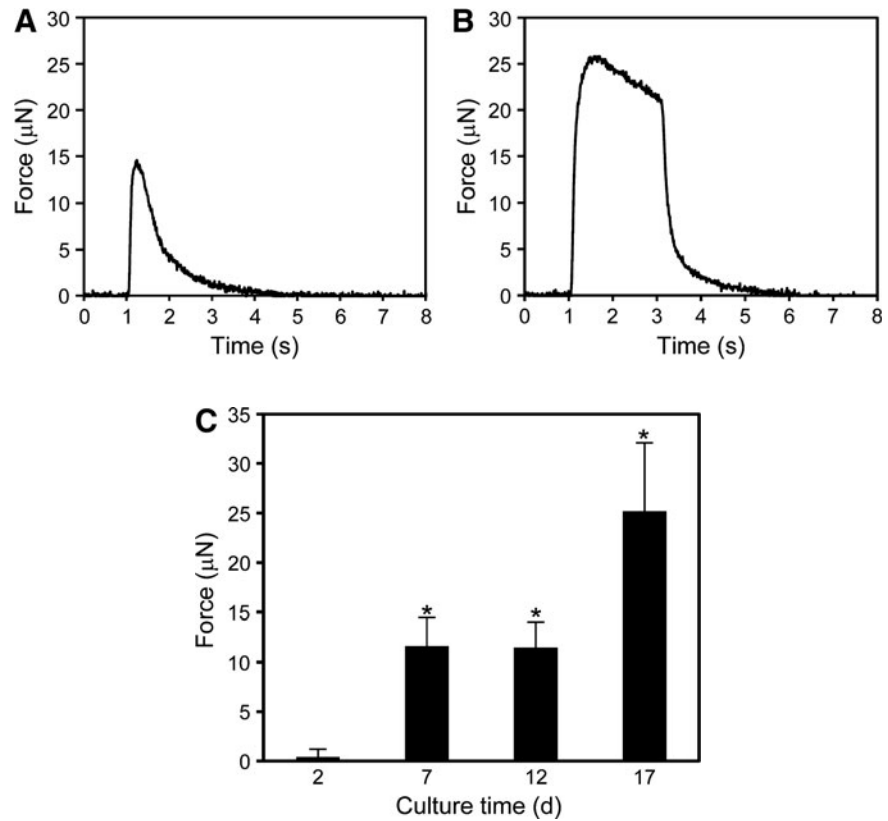
**FIG. 3.** Expression profiles of muscle-specific proteins in artificial tissue constructs during differentiation. **(A)** Western blot analysis for myogenin, MHC, tropomyosin, and GAPDH. **(B)** Creatine kinase activity. The data are expressed as mean  $\pm$  SD of three constructs. \* $p < 0.05$  against day 0.

number of nuclei decreased (Fig. 2A). After this, creatine kinase activity of the artificial tissue construct was measured. Creatine kinase is involved in energy metabolism of muscle tissues during muscle contraction.<sup>23</sup> As shown in Figure 3B, creatine kinase activity increased from day 2 and continued to increase throughout the culture period. It has been reported that proliferative myoblasts differentiate into myocytes, thereby inducing myogenin expression by cell cycle withdrawal, which subsequently leads to the expression of muscle-specific proteins, such as MHC, tropomyosin, and creatine kinase.<sup>24</sup> Thus, the expression pattern of muscle-specific proteins in the artificial tissue construct was consistent with expression in the normal myogenesis pathway.

#### Contractile properties of artificial skeletal muscle tissues

To evaluate contractile properties, the artificial skeletal muscle constructs were stimulated with electrical pulses. In response to the pulses applied, the tissue constructs contracted to generate a physical force. Twitching responses were elicited using a single electrical pulse (voltage, 15 V; width, 10 ms) and tetanus responses were measured by stimulation with electric pulses (voltage, 15 V; width, 10 ms; frequency, 50 Hz; duration, 2 s). The force generation profiles in response to the electrical stimulation required to induce

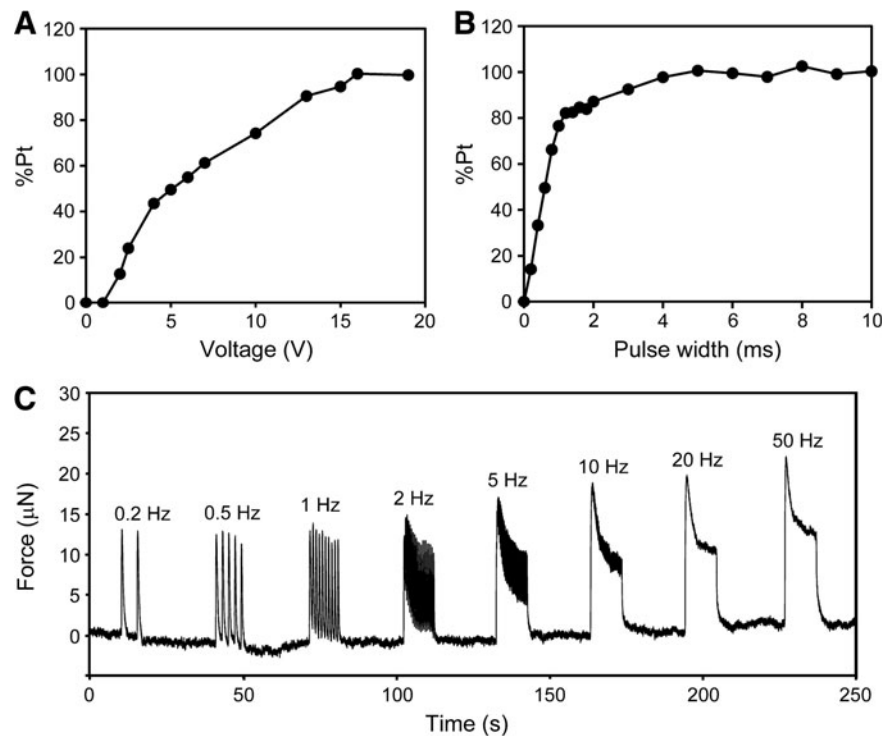
**FIG. 4.** Contractile properties of artificial tissue constructs. **(A)** A representative peak of the twitch force generated by the artificial tissue construct (day 7), using a single electric pulse (voltage, 15 V; width, 10 ms). **(B)** Fusion of tetanus of the artificial tissue construct (day 7), stimulated with multiple electric pulses (voltage, 15 V; width, 10 ms; frequency, 50 Hz; duration, 2 s). **(C)** Maximum twitch force of artificial tissue constructs during differentiation (voltage, 15 V; width, 10 ms). The data are expressed as mean  $\pm$  SD of three constructs. \* $p < 0.05$  against day 2.



twitch and fused tetanus responses are shown in Figure 4A and 4B, respectively. Both profiles of the artificial tissue construct were very similar to those of natural adult muscles, although the force levels were much lower.<sup>25,26</sup> Figure 4C shows the maximum contractile forces of the artificial tissue constructs during culture in the differentiation medium. The

tissue constructs did not generate obvious contractile forces ( $0.4 \pm 0.7 \mu$ N) on day 2. As muscle differentiation progressed within the tissue construct, the contractile force generated by electrical stimulation became progressively stronger. This response coincided with the expression patterns of muscle-specific proteins (Fig. 3).

**FIG. 5.** Excitability of artificial tissue constructs. **(A)** Rheobase of the artificial tissue construct (day 7). Using a 10-ms pulse width, the voltage was incrementally increased from zero. As the voltage is increased, the twitch force increases correspondingly. The twitch force plateau was defined as 100% of peak twitch force (Pt), and the voltage at 50% Pt was determined as rheobase. **(B)** Chronaxie of the artificial tissue construct (day 7). The voltage was set to twofold of the rheobase, and the pulse width was incrementally increased to measure the percentage of peak twitch force. The pulse width at 50% Pt was determined as chronaxie. **(C)** Force–frequency diagram for the artificial tissue construct. Electric pulses (voltage, 15 V; width, 10 ms; train duration, 10 s) with various frequencies in the range of 0.2–50 Hz were applied to the tissue construct, and twitch forces were monitored.



A series of pulses with variable voltages and width were applied to determine the excitability of the artificial tissue constructs. The effect of voltage (Fig. 5A) and pulse width (Fig. 5B) on twitch force generation were measured to determine the excitability in terms of rheobase and chronaxie. Lower values of both rheobase and chronaxie indicate greater excitability of muscle tissues. The artificial tissue constructs exhibited a rheobase of  $4.45 \pm 0.65$  V (Fig. 5A) and chronaxie of  $0.72 \pm 0.09$  ms (Fig. 5B).

In this study, the artificial skeletal muscle tissue constructs fabricated by Mag-TE successfully contracted in response to electric pulses. As shown in Figure 4C, the tissue constructs generated a maximum twitch force of  $33.2 \mu\text{N}$  ( $1.06 \text{ mN/mm}^2$ ), which corresponds to  $\sim 0.5\%$  of adult mammalian skeletal muscle ( $210 \text{ mN/mm}^2$ ).<sup>25,26</sup> In addition, the chronaxie of the tissue constructs was 0.72 ms, which indicated a lower excitability than that of normal skeletal muscle (0.1–0.3 ms).<sup>27</sup> The low active tension and excitability may be attributable to the presence of nondifferentiated myoblasts within the tissue constructs (Fig. 1D) or the presence of myotubes that are unresponsive to electrical pulses.<sup>28</sup> Multiple central nuclei were observed within myotubes of the constructs on day 7 (Fig. 1E) and day 17 (data not shown), suggesting that the tissue construct was still immature. Previous reports indicate that continuous stimulation by electrical pulses<sup>28</sup> or mechanical stretching<sup>29</sup> enhance myogenesis of myoblast cells. These results suggest that to mimic natural skeletal muscle development and maturation, both the biological milieu and physical stimuli should be introduced to skeletal muscle tissue engineering using myoblast cell lines. Nevertheless, the artificial tissue constructs fabricated from proliferative myoblast cells in this study exhibited skeletal muscle function.

The frequency characteristics of myotubes in an electric field have not been previously described in detail. Marotta *et al.*<sup>30</sup> reported that myotubes contract rhythmically with electric pulses between 1 and 5 Hz under phase-contrast microscopy, while Yamasaki *et al.*<sup>27</sup> quantified myotube contraction based on cell image analysis. However, there are a few reports on the evaluation of frequency characteristics of muscle tissues by quantifying force generation. A force-frequency diagram for the artificial tissue construct is shown in Figure 5C. The tissue contracted rhythmically in response to low-frequency electrical pulses with short intervals. This result indicates that the artificial tissue constructs are applicable to electrically controlled bioactuators. Moreover, similar to natural skeletal muscle tissues, individual twitch contractions occurred by low-frequency electrical stimulation, whereas the additional activation of contractile elements, named tetanus, was observed by repeated stimulation with a higher frequency (Fig. 5C). Thus, the apparatus developed in this study was useful for the measurement of contractile properties. These results indicate that the properties of the artificial tissue constructs were qualitatively very similar to those of natural skeletal muscle tissues, although the force levels of the artificial tissues were considerably low.

## Conclusion

In the present study, we evaluated the biochemical and contractile properties of artificial skeletal muscle tissue constructs fabricated by Mag-TE. The tissue constructs ex-

pressed myogenic markers during the differentiation stages and contracted to generate physical forces in response to electrical stimulation. The expression profiles of myogenic markers (myogenin, MHC, tropomyosin, and creatine kinase) correlated well with the contractile properties of the tissue constructs. These results indicate that the artificial skeletal muscle tissue constructs fabricated in this study were physiologically functional, and the data for evaluating the functional properties may provide useful information for skeletal muscle tissue engineering.

## Acknowledgments

One of the authors (Y.Y.) is a research fellow of the Japan Society for the Promotion of Science (JSPS). This work was supported in part by Grants-in-Aid for Scientific Research (nos. 21686079 and 22-2293) of JSPS.

## Disclosure Statement

No competing financial interests exist.

## References

1. Law, P.K., Goodwin, T.G., Fang, Q., Deering, M.B., Dugirala, V., Larkin, C., Florendo, J.A., Kirby, D.S., Li, H.J., and Chen, M. Cell transplantation as an experimental treatment for Duchenne muscular dystrophy. *Cell Transplant* **2**, 485, 1993.
2. Allen, R.E., Temm-Grove, C.J., Sheehan, S.M., and Rice, G. Skeletal muscle satellite cell cultures. *Methods Cell Biol* **52**, 155, 1997.
3. Yan, W., George, S., Fotadar, U., Tyhovych, N., Kamer, A., Yost, M.J., Price, R.L., Haggart, C.R., Holmes, J.W., and Terracio, L. Tissue engineering of skeletal muscle. *Tissue Eng* **13**, 2781, 2007.
4. Yaffe, D., and Saxel, O. Serial passaging and differentiation of myogenic cells isolated from dystrophic mouse muscle. *Nature* **270**, 725, 1977.
5. Herr, H., and Dennis, R.G. A swimming robot actuated by living muscle tissue. *J Neuroeng Rehabil* **1**, 6, 2004.
6. Morishima, K., Tanaka, Y., Ebara, M., Shimizu, T., Kikuchi, A., Yamato, M., Okano, T., and Kitamori, T. Demonstration of a bio-microactuator powered by cultured cardiomyocytes coupled to hydrogel micropillars. *Sens Actuator B Chem* **119**, 345, 2006.
7. Akiyama, Y., Iwabuchi, K., Furukawa, Y., and Morishima, K. Long-term and room temperature operable bioactuator powered by insect dorsal vessel tissue. *Lab Chip* **9**, 140, 2009.
8. Feinberg, A.W., Feigel, A., Shevkoplyas, S.S., Sheehy, S., Whitesides, G.M., and Parker, K.K. Muscular thin films for building actuators and powering devices. *Science* **317**, 1366, 2007.
9. Tanaka, Y., Morishima, K., Shimizu, T., Kikuchi, A., Yamato, M., Okano, T., and Kitamori, T. An actuated pump on-chip powered by cultured cardiomyocytes. *Lab Chip* **6**, 362, 2006.
10. Okano, T., and Matsuda, T. Tissue engineered skeletal muscle: preparation of highly dense, highly oriented hybrid muscular tissues. *Cell Transplant* **7**, 71, 1998.
11. Giraud, M.N., Ayuni, E., Cook, S., Siepe, M., Carrel, T.P., and Tevæarai, H.T. Hydrogel-based engineered skeletal muscle grafts normalize heart function early after myocardial infarction. *Artif Organs* **32**, 692, 2008.
12. Dennis, R.G., and Kosnik, P.E. 2nd. Excitability and isometric contractile properties of mammalian skeletal muscle

- constructs engineered *in vitro*. *In Vitro Cell Dev Biol Anim* **36**, 327, 2000.
13. Ito, A., Hayashida, M., Honda, H., Hata, K., Kagami, H., Ueda, M., and Kobayashi, T. Construction and harvest of multilayered keratinocyte sheets using magnetite nanoparticles and magnetic force. *Tissue Eng* **10**, 873, 2004.
  14. Ito, A., Shinkai, M., Honda, H., and Kobayashi, T. Medical application of functionalized magnetic nanoparticles. *J Biosci Bioeng* **100**, 1, 2005.
  15. Yamamoto, Y., Ito, A., Kato, M., Kawabe, Y., Shimizu, K., Fujita, H., Nagamori, E., and Kamihira, M. Preparation of artificial skeletal muscle tissues by a magnetic force-based tissue engineering technique. *J Biosci Bioeng* **108**, 538, 2009.
  16. Akiyama, H., Ito, A., Kawabe, Y., and Kamihira, M. Genetically engineered angiogenic cell sheets using magnetic force-based gene delivery and tissue fabrication techniques. *Biomaterials* **31**, 1251, 2010.
  17. Shinkai, M., Yanase, M., Honda, H., Wakabayashi, T., Yoshida, J., and Kobayashi, T. Intracellular hyperthermia for cancer using magnetite cationic liposomes: *in vitro* study. *Jpn J Cancer Res* **87**, 1179, 1996.
  18. Yoshiko, Y., Hirao, K., and Maeda, N. Differentiation in C2C12 myoblasts depends on the expression of endogenous IGFs and not serum depletion. *Am J Physiol Cell Physiol* **283**, C1278, 2002.
  19. Akiyama, H., Ito, A., Kawabe, Y., and Kamihira, M. Fabrication of complex three-dimensional tissue architectures using a magnetic force-based cell patterning technique. *Biomed Microdevices* **11**, 713, 2009.
  20. Nakanishi, K., Dohmae, N., and Morishima, N. Endoplasmic reticulum stress increases myofiber formation *in vitro*. *FASEB J* **21**, 2994, 2007.
  21. Hasty, P., Bradley, A., Morris, J.H., Edmondson, D.G., Venuti, J.M., Olson, E.N., and Klein, W.H. Muscle deficiency and neonatal death in mice with a targeted mutation in the myogenin gene. *Nature* **364**, 501, 1993.
  22. Chargé, S.B., and Rudnicki, M.A. Cellular and molecular regulation of muscle regeneration. *Physiol Rev* **84**, 209, 2004.
  23. Bessman, S.P., and Geiger, P.J. Transport of energy in muscle: the phosphorylcreatine shuttle. *Science* **211**, 448, 1981.
  24. Andrés, V., and Walsh, K. Myogenin expression, cell cycle withdrawal, and phenotypic differentiation are temporally separable events that precede cell fusion upon myogenesis. *J Cell Biol* **132**, 657, 1996.
  25. Close, R.I. Dynamic properties of mammalian skeletal muscles. *Physiol Rev* **52**, 129, 1972.
  26. Isaacson, A., Hinkes, M.J., and Taylor, S.R. Contracture and twitch potentiation of fast and slow muscles of the rat at 20 and 37 C. *Am J Physiol* **218**, 33, 1970.
  27. Yamasaki, K., Hayashi, H., Nishiyama, K., Kobayashi, H., Uto, S., Kondo, H., Hashimoto, S., and Fujisato, T. Control of myotube contraction using electrical pulse stimulation for bio-actuator. *J Artif Organs* **12**, 131, 2009.
  28. Fujita, H., Nedachi, T., and Kanzaki, M. Accelerated *de novo* sarcomere assembly by electric pulse stimulation in C2C12 myotubes. *Exp Cell Res* **313**, 1853, 2007.
  29. Powell, C.A., Smiley, B.L., Mills, J., and Vandenberg, H.H. Mechanical stimulation improves tissue-engineered human skeletal muscle. *Am J Physiol Cell Physiol* **283**, C1557, 2002.
  30. Marotta, M., Bragós, R., and Gómez-Foix, A.M. Design and performance of an electrical stimulator for long-term contraction of cultured muscle cells. *BioTechniques* **36**, 68, 2004.

Address correspondence to:

Masamichi Kamihira, Ph.D.

Department of Chemical Engineering

Faculty of Engineering

Kyushu University

744 Motooka, Nishi-ku

Fukuoka 819-0395

Japan

E-mail: kamihira@chem-eng.kyushu-u.ac.jp

Received: May 26, 2010

Accepted: July 29, 2010

Online Publication Date: September 7, 2010

Reproduced with permission of the copyright owner. Further reproduction prohibited without permission.